

PROPERTIES OF ROBUST MIMO DETECTOR

C. Y. Chong¹, F. Pascal¹, J-P. Ovarlez^{1,2}, M. Lesturgie^{1,2}

¹ SONDRRA, Supelec
3 rue Joliot-Curie
91192 Gif-sur-Yvette Cedex, France
phone: + 33 1 6985 1813, fax: + 33 1 6985 1809
chinyuan.chong@supelec.fr

² ONERA-DEMR
Chemin de la Hunière,
91761 Palaiseau Cedex, France

ABSTRACT

Previously, using the Maximum Likelihood (ML) method, we obtained a new Gaussian Multiple-Input Multiple-Output (MIMO) detector which is robust to the correlation between the subarrays [1]. It is found that this new detector has the same statistical properties in the absence of target irregardless if the subarrays are correlated or not. It becomes the MIMO Optimum Gaussian Detector (OGD) [2, 3] when the subarrays are uncorrelated. In this paper, we define two main configurations, transmit or receive diversity, with varying degree of freedoms (subarrays). Using these configurations, we study the detection performance of this detector and its adaptive version with respect to various parameters.

1. INTRODUCTION

In the context of radar, a statistical Multiple-Input Multiple-Output (MIMO) radar is one where both the transmit and receive elements are sufficiently separated so as to provide spatial diversity. This reduces the fluctuations of the target Radar Cross Section (RCS) due to the different target aspects seen by each pair of transmit-receive elements. It can also be used to improve the probability of detection and resolutions. On top of that, each transmit element sends a different (orthogonal) waveform which can be separated at the receive end. This provides waveform diversity which in turn increases the separation between clutter and target returns.

Assuming that all the subarrays are uncorrelated, the optimum detector under Gaussian clutter is the MIMO Optimum Gaussian Detector (MIMO OGD) [2, 3]. According to [2], the subarrays have to be sufficiently spaced in order to decorrelate the signal returns in each subarray. It might not be possible to respect this condition, especially when we consider MIMO-STAP where the transmit and/or receive subarrays are moving. Moreover, perfectly orthogonal waveforms do not exist, especially in the presence of Doppler frequency. We assume that insufficient spacing between subarrays and imperfect orthogonality of the transmitted waveforms introduce correlation between the subarrays.

Under this context, we obtained a new Gaussian MIMO detector which is robust to the correlation between subarrays [1]. It is found that this new detector has the same statistical properties in the absence of target irregardless if the subarrays are correlated or not. It becomes the MIMO OGD when the subarrays are uncorrelated. Due to its robustness, we will denote it as Robust-MIMO (R-MIMO) detector.

The following signal model that takes into account the correlation of the different subarrays has been used:

$$\mathbf{y} = \mathbf{P}\boldsymbol{\alpha} + \mathbf{z},$$

where the vectors \mathbf{y} , $\boldsymbol{\alpha}$ and \mathbf{z} are the concatenation of all the received signals, target RCS and clutter returns, respectively:

$$\mathbf{y} = \begin{bmatrix} \mathbf{y}_1 \\ \vdots \\ \mathbf{y}_K \end{bmatrix}, \quad \boldsymbol{\alpha} = \begin{bmatrix} \alpha_1 \\ \vdots \\ \alpha_K \end{bmatrix}, \quad \mathbf{z} = \begin{bmatrix} \mathbf{z}_1 \\ \vdots \\ \mathbf{z}_K \end{bmatrix},$$

where K is the effective number of subarrays, α_i is the RCS of the target seen by the i -th subarray. \mathbf{z}_i is the $L_i \times 1$ clutter vector and L_i is the effective number of elements in the i -th subarray. \mathbf{P} is the $(\sum_{i=1}^K L_i) \times K$ matrix containing all the steering vectors:

$$\mathbf{P} = \begin{bmatrix} \mathbf{p}_1 & & \mathbf{0} \\ & \ddots & \\ \mathbf{0} & & \mathbf{p}_K \end{bmatrix},$$

and \mathbf{p}_i is the $L_i \times 1$ steering vector for the i -th subarray.

The covariance matrix of each \mathbf{z}_i is given by \mathbf{M}_{ii} while the inter-correlation matrix between \mathbf{z}_i and \mathbf{z}_j is denoted as \mathbf{M}_{ij} such that $\mathbf{z} \sim \mathcal{CN}(\mathbf{0}, \mathbf{M})$ where \sim means to be distributed as and \mathcal{CN} denotes the complex normal distribution.

Remark 1.1. *This signal model is of a so-called hybrid configuration, i.e. it can have the characteristics of both the classical phased array radar and the fully statistical MIMO radar. It includes also both radars as special cases.*

In this paper, we recap the R-MIMO detector as well as its adaptive version. Based on this detector, we discuss several parameters and their effects on performance detection. Using several different configurations, Monte-Carlo simulations are then done to validate the results.

This paper is organized as follows. Firstly, we recap the R-MIMO detector and its statistical properties in the beginning of Section 2. We then identify several parameters and discuss their effects on detection performance (Section 2.2). Some simulations results are presented in Section 2.3. Next, in Section 3, we consider the adaptive version of this new detector which has been derived based on the Kelly's Test [4]. Due to the estimation of the covariance matrix, there is a loss factor, b which we will discuss briefly in Section 3.2. Simulation results are then presented in Section 3.3. Finally, the results are summarized in Section 4.

The authors would like to thank DSO National Laboratories (Singapore) for funding this project.

2. ROBUST MIMO DETECTOR

The robust MIMO (R-MIMO) detector is given by [1]:

$$\ln \Lambda(\mathbf{y}) = \mathbf{y}^\dagger \mathbf{M}^{-1} \mathbf{P} (\mathbf{P}^\dagger \mathbf{M}^{-1} \mathbf{P})^{-1} \mathbf{P}^\dagger \mathbf{M}^{-1} \mathbf{y} \underset{H_0}{\overset{H_1}{\geq}} \lambda.$$

2.1 Statistical Properties

As shown in [1], $\mathbf{y} \sim \mathcal{CN}(\mathbf{0}, \mathbf{M})$ under H_0 and the distribution of the detector is simply the central chi-square with $2K$ degrees of freedom, denoted by $\chi_{2K}^2(0)$. This is the same as the distribution of the MIMO OGD detector where the subarrays are not correlated. Under H_1 , $\mathbf{y} \sim \mathcal{CN}(\mathbf{P}\boldsymbol{\alpha}, \mathbf{M})$ and the distribution of the detector becomes the non-central chi-square with $2K$ degrees of freedom and a non-centrality parameter of $2\boldsymbol{\alpha}^\dagger \mathbf{P}^\dagger \mathbf{M}^{-1} \mathbf{P} \boldsymbol{\alpha}$, denoted by $\chi_{2K}^2(2\boldsymbol{\alpha}^\dagger \mathbf{P}^\dagger \mathbf{M}^{-1} \mathbf{P} \boldsymbol{\alpha})$.

Note that the distribution does not depend on the correlation between the subarrays, showing the M-Constant False Alarm Rate (M-CFAR) property of the R-MIMO OGD detector. This property is very useful as it means that the requirement of independence between subarrays can be relaxed for some applications, e.g. the regulation of false alarms.

2.2 Discussion

K - effective number of subarrays

Let there be \tilde{N} transmit subarrays and \tilde{M} receive subarrays. Due to waveform diversity, the effective number of subarrays is given by: $K = \tilde{N}\tilde{M}$. It determines the degree of freedom in the distribution of the detector. Given the same Signal-to-Noise Ratio (SNR), detection performance deteriorates with increasing degree of freedom, as a higher threshold λ is required to maintain the same P_{fa} (see Appendix A). However, with fewer subarrays, SNR can vary greatly due to the fluctuations of the target RCS. Hence the choice of K will depend on the applications, e.g. large K for surveillance and small K for direction finding.

N_e - effective number of elements

Consider that the n -th transmit and m -th receive subarray contain N_n and M_m elements, respectively, for $n = 1, \dots, \tilde{N}$ and $m = 1, \dots, \tilde{M}$. The physical number of elements is given by $N = \sum_{n=1}^{\tilde{N}} N_n + \sum_{m=1}^{\tilde{M}} M_m$. The effective number of elements in each subarray is $L_i = N_n M_m$ while the effective number of elements is given by $N_e = \sum_{i=1}^K L_i$. One of the advantages of transmit diversity in MIMO is that it can increase the effective number of elements such that it is greater than the physical number of elements, N .

SNR gain is defined to be:

$$\begin{aligned} SNR_g &= \frac{SNR_{post}}{SNR_{pre}}, \\ &= \frac{\boldsymbol{\alpha}^\dagger \mathbf{P}^\dagger \mathbf{M}^{-1} \mathbf{P} \boldsymbol{\alpha}}{\frac{|\alpha|_{ave}^2}{\sigma^2}}, \\ &= \frac{\boldsymbol{\alpha}^\dagger \mathbf{P}^\dagger \mathbf{M}_{norm}^{-1} \mathbf{P} \boldsymbol{\alpha}}{|\alpha|_{ave}^2}, \\ &\approx \frac{\sum_{i=1}^K L_i |\alpha|_{ave}^2}{|\alpha|_{ave}^2} = N_e, \end{aligned}$$

where SNR_{pre} and SNR_{post} are the pre- and post-processing SNR, respectively. $|\alpha|_{ave}^2 = \frac{\boldsymbol{\alpha}^\dagger \boldsymbol{\alpha}}{K}$ and $\mathbf{M} = \sigma^2 \mathbf{M}_{norm}$. Note that the non-centrality parameter in the distribution of the detector under H_1 is $2SNR_{post}$. The factor 2 comes from the fact that the clutter power is divided equally between its real and imaginary part such that it is halved for each degree of freedom.

Remark 2.1. SNR gain is proportional to N_e . This gain comes from the coherent processing gain within the subarrays.

2.2.1 Multiple-Input Single-Output (MISO) Case

Consider the Multiple-Input Single-Output (MISO) case where there are K widely-spaced transmit elements and one single receive array with L elements. Keeping the total number of elements, N to be the same, if there are more transmit elements (thus creating more effective subarrays), there will be fewer elements in the receive array. This affects the effective total number of elements which in turn affects the SNR gain.

2.2.2 Single-Input Multiple-Output (SIMO) Case

On the other hand, consider the Single-Input Multiple-Output (SIMO) case where there is only 1 transmit element. The spatial diversity comes only from the receive subarrays. With N total number of elements, there are $L = \frac{N-1}{K}$ elements in each receive subarray (where $\frac{N-1}{K}$ is an integer). Hence the effective total number of elements remains the same for different K . Note that $N_e = N - 1$ in this case.

The variation of N_e with K for both cases (MISO and SIMO) is shown in Fig. 1.

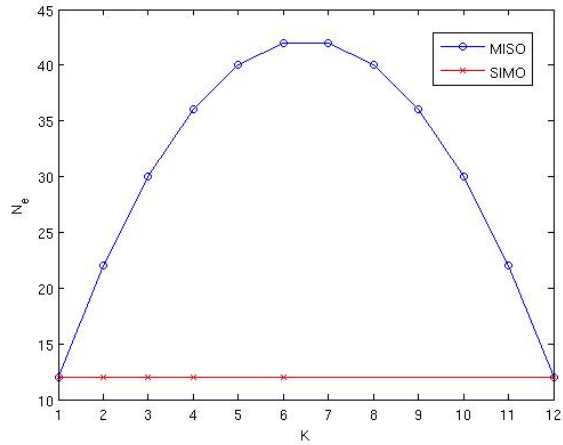


Figure 1: Variation of N_e with K for MISO and SIMO cases. $N = 13$.

2.3 Simulation Results

For the simulations in this paper, the covariance matrix \mathbf{M}_{i_i} of each \mathbf{z}_i , without loss of generalities, is chosen identically and equal to \mathbf{M}_{sa} . \mathbf{M}_{sa} is spatially colored and its elements are given by:

$$\mathbf{M}_{sa}(p, q) = \rho^{|p-q|} e^{j\frac{\pi}{2}(p-q)}.$$

The correlation coefficient ρ is chosen to be 0.2 such that there is a slight correlation between different elements of the subarray. The subarrays are set to be correlated and the inter-correlation matrices are generated using uniformly distributed variables:

$$M_{ij}(p, q) = \tau_{ij} \rho_{ij}^{|p-q|} e^{j\frac{\pi}{2}(p-q)},$$

where ρ_{ij} is uniformly distributed in the interval $[0, 0.4]$ such that the mean of ρ_{ij} is equal to ρ . The inclusion of τ_{ij} is to make the power of the intercorrelation matrices M_{ij} smaller than that of the correlation matrices M_{ii} and it is uniformly distributed in the interval $[0, 0.1]$.

In Fig. 2, the Probability of Detection (P_d) against SNR_{pre} (dash-dotted lines) and SNR_{post} (solid lines) are plotted for $K=3, 6, 12$ and $N=13$ for the SIMO case. Here, the effective number of elements remains the same. Hence the SNR gain is basically the same for all K . However, with increasing degrees of freedom, the detection performance degrades.

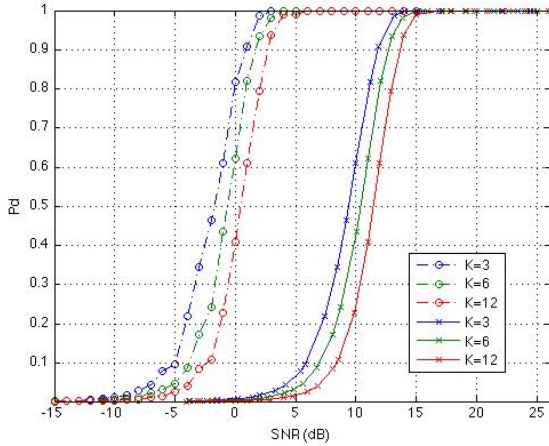


Figure 2: P_d against SNR_{pre} (dash-dotted lines) and SNR_{post} (solid lines) under Gaussian clutter for correlated subarrays. $P_{fa} = 10^{-3}$. SIMO case.

In Fig. 3, P_d against SNR_{pre} (dash-dotted lines) and SNR_{post} (solid lines) are plotted for $K=3, 6, 12$ and $N=13$ for the MISO case. Here, the effective number of elements N_e changes depending on K . From Fig. 1, we see that N_e for $K=6$ is better than that for $K=3$. Indeed, we see that the detection performance for $K=6$ becomes better after taking into consideration processing gains.

3. ADAPTIVE MIMO DETECTOR

As the covariance matrix is usually unknown in reality, we consider in this section the adaptive version of the detector. As derived in [1] based on Kelly's Test [4], the optimum adaptive detector is given by:

$$\hat{\Lambda}(\mathbf{y}) = \frac{\mathbf{y}^\dagger \hat{\mathbf{M}}^{-1} \mathbf{P} (\mathbf{P}^\dagger \hat{\mathbf{M}}^{-1} \mathbf{P})^{-1} \mathbf{P}^\dagger \hat{\mathbf{M}}^{-1} \mathbf{y}}{N_r + \mathbf{y}^\dagger \hat{\mathbf{M}}^{-1} \mathbf{y}} \underset{H_0}{\underset{H_1}{\geq}} \eta, \quad (1)$$

where $\hat{\mathbf{M}}$ is the Sample Covariance Matrix of \mathbf{M} and is given by:

$$\hat{\mathbf{M}} = \frac{1}{N_r} \sum_{l=1}^{N_r} \mathbf{c}(l) \mathbf{c}(l)^\dagger.$$

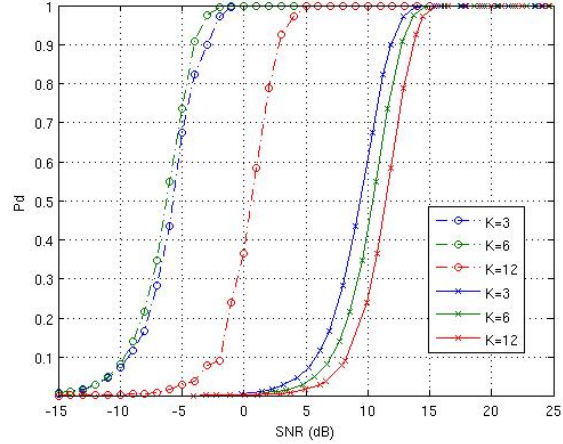


Figure 3: P_d against SNR_{pre} (dash-dotted lines) and SNR_{post} (solid lines) under Gaussian clutter for correlated subarrays. $P_{fa} = 10^{-3}$. MISO case.

$\mathbf{c}(l)$ are target-free secondary data which are assumed to be independent and identically distributed and N_r is the number of secondary data.

3.1 Statistical Properties

According to [5], the distribution of the adaptive version is:

$$\hat{\Lambda}(\mathbf{y}) \stackrel{d}{=} \begin{cases} H_0: & \beta_{K, N_r - N_e + 1}(0), \\ H_1: & \beta_{K, N_r - N_e + 1}(\gamma), \end{cases}$$

where $\beta_{K, N_r - N_e + 1}$ is the beta-distributed random variable (r.v.) with parameters K and $N_r - N_e + 1$. The beta-distributed r.v. is central under H_0 and non-central with non-centrality parameter γ under H_1 . γ is conditional on b which is also beta-distributed with parameters $N_r - N_e + K + 1$ and $N_e - K$:

$$\gamma = 2SNR_{post} \cdot b \quad b \sim \beta_{N_r - N_e + K + 1, N_e - K}. \quad (2)$$

b can be considered as a loss factor on SNR_{post} due to the estimation of the covariance matrix.

Theorem 3.1. *In the case where there is only 1 effective element per subarray such that $N_e = K$, the loss factor becomes 1 and the non-centrality parameter is simply:*

$$\gamma = 2SNR_{post}.$$

Proof. When there is only 1 element per subarray, $\mathbf{P} = \mathbf{I}$ and Eqn. (1) becomes:

$$\begin{aligned} \hat{\Lambda}(\mathbf{y}) &= \frac{\mathbf{y}^\dagger \hat{\mathbf{M}}^{-1} \mathbf{y}}{N_r + \mathbf{y}^\dagger \hat{\mathbf{M}}^{-1} \mathbf{y}}, \\ &= \frac{\mathbf{y}^\dagger \bar{\mathbf{M}}^{-1} \mathbf{y}}{1 + \mathbf{y}^\dagger \bar{\mathbf{M}}^{-1} \mathbf{y}}, \end{aligned}$$

where $\bar{\mathbf{M}} = N_r \hat{\mathbf{M}} \sim \mathcal{CW}(N_r, N_e, \mathbf{M})$ and \mathcal{CW} denotes the complex Wishart distribution.

Let us define the matrix $\mathbf{C} = \mathbf{M}^{-1/2} \bar{\mathbf{M}} \mathbf{M}^{-1/2}$. According to [6], $\mathbf{C} \sim \mathcal{CW}(N_r, N_e, \mathbf{I})$. Consider the whitened signal

$\mathbf{x} = \mathbf{M}^{-1/2}\mathbf{y}$, we next perform an unitary transformation on \mathbf{x} by \mathbf{V} which is defined as:

$$\mathbf{V} = \left[\frac{\mathbf{x}}{\sqrt{\mathbf{x}^\dagger \mathbf{x}}}, \tilde{\mathbf{V}} \right],$$

where $\tilde{\mathbf{V}}^\dagger \mathbf{x} = \mathbf{0}$. The transformed variable can be expressed using $\mathbf{e}_1^\dagger = [1 \ 0 \ \dots \ 0]$:

$$\mathbf{V}^\dagger \mathbf{x} = \sqrt{\mathbf{x}^\dagger \mathbf{x}} \mathbf{e}_1$$

and the detector becomes:

$$\begin{aligned} \hat{\Lambda}(\mathbf{x}) &= \frac{\mathbf{x}^\dagger \mathbf{x} \mathbf{e}_1^\dagger \mathbf{G}^{-1} \mathbf{e}_1}{1 + \mathbf{x}^\dagger \mathbf{x} \mathbf{e}_1^\dagger \mathbf{G}^{-1} \mathbf{e}_1}, \\ &= \frac{\mathbf{x}^\dagger \mathbf{x} g_{11}}{1 + \mathbf{x}^\dagger \mathbf{x} g_{11}}, \end{aligned}$$

where $\mathbf{G} = \mathbf{V}^\dagger \mathbf{C} \mathbf{V} \sim \mathcal{CW}(N_r, N_e, \mathbf{I})$ and g_{11} is the top left element of \mathbf{G}^{-1} . Using Theorem 1 in [5], we find that the distribution of g_{11} is $\chi_{2(N_r - N_e + 1)}^2$ and it is independent from \mathbf{x} .

Under H_0 , $\mathbf{x} \sim \mathcal{CN}(\mathbf{0}, \mathbf{I})$ such that $\mathbf{x}^\dagger \mathbf{x} \sim \chi_{2N_e}^2(0) = \chi_{2K}^2(0)$. Under H_1 , $\mathbf{x} \sim \mathcal{CN}(\mathbf{M}^{-1/2} \boldsymbol{\alpha}, \mathbf{I})$ such that $\mathbf{x}^\dagger \mathbf{x} \sim \chi_{2K}^2(2\boldsymbol{\alpha}^\dagger \mathbf{M}^{-1} \boldsymbol{\alpha}) = \chi_{2K}^2(2SNR_{post})$. Hence the distribution of the detector can be described as:

$$\hat{\Lambda}(\mathbf{y}) \stackrel{d}{=} \begin{cases} H_0: & \beta_{K, N_r - N_e + 1}(0) \\ H_1: & \beta_{K, N_r - N_e + 1}(2SNR_{post}) \end{cases}$$

Therefore, b is equal to one. \square

3.2 Discussion

b - loss factor

The mean value of the loss factor, b , for receive and transmit diversity cases, respectively is plotted in Fig. 4. $b \in [0, 1]$ and there is no SNR loss if $b=1$. $L_r = \frac{N_r}{N_e}$ is the number of times N_r is greater than N_e . Note that for the SIMO case, there are some values of K that are not possible as it will result in non-integral number of elements in each subarray.

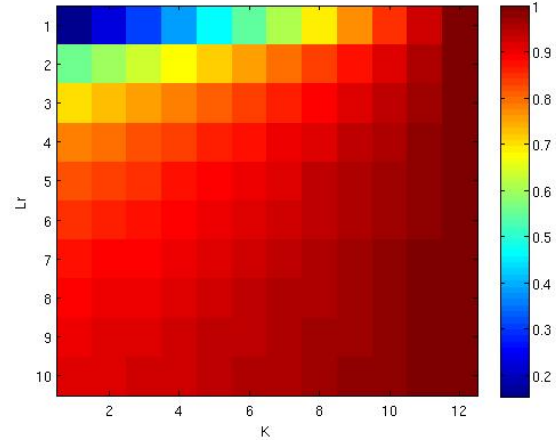
As expected, with $L_r=2$, we have $\text{mean}(b) \approx 0.5$ which is roughly equivalent to the well-known 3dB loss case. The loss factor becomes bigger (less loss) with increasing number of subarrays, K . The SIMO case has bigger loss factor in general.

3.3 Simulation Results

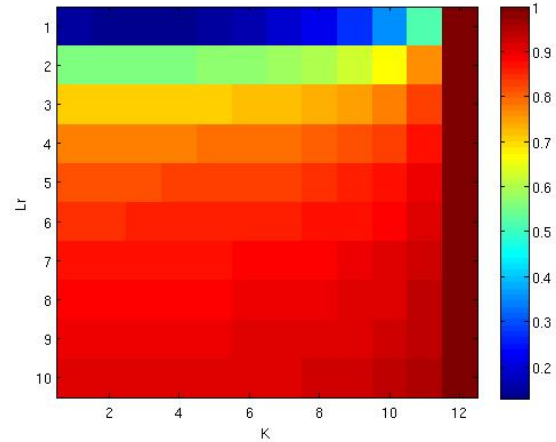
In Fig. 5, we have P_d against SNR_{pre} for different K , $L_r=3$ and $N=13$. This is for the MISO case. As expected, we have the best performance when the effective number of element is largest (see Fig. 1). However, note that more secondary data are required to ensure $L_r=2$ when N_e is large.

Staying in the MISO case, we have P_d against SNR_{pre} for different L_r , $K=6$ and $N=13$ in Fig. 6. We see that the minimum number of secondary data required is $L_r=2$. While the detection performance improves with increasing L_r , the improvement is no longer significant for $L_r > 4$.

Fig. 7 shows a slice of Fig. 5 ($K=6$) and Fig. 6 ($L_r=3$).



(a) SIMO case



(b) MISO case

Figure 4: Mean value of loss factor b against K and L_r .

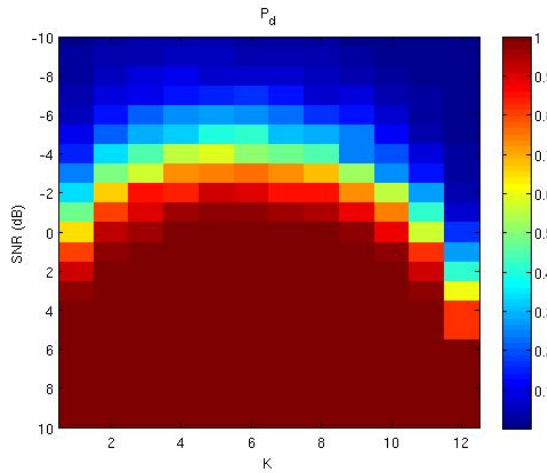


Figure 5: P_d against SNR_{pre} and K under Gaussian clutter for correlated subarrays. $P_{fa} = 10^{-3}$, $L_r = 3$ and $N = 13$. MISO case.

4. CONCLUSIONS

In this paper, we studied the properties of the new R-MIMO detector which takes into consideration possible correlation

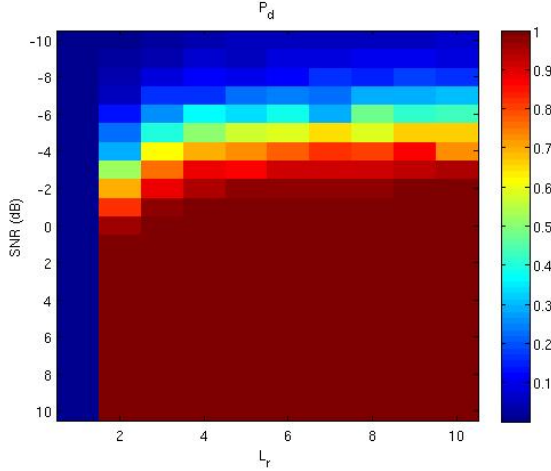


Figure 6: P_d against SNR_{pre} and L_r under Gaussian clutter for correlated subarrays. $P_{fa} = 10^{-3}$ and $K = 6$. MISO case.

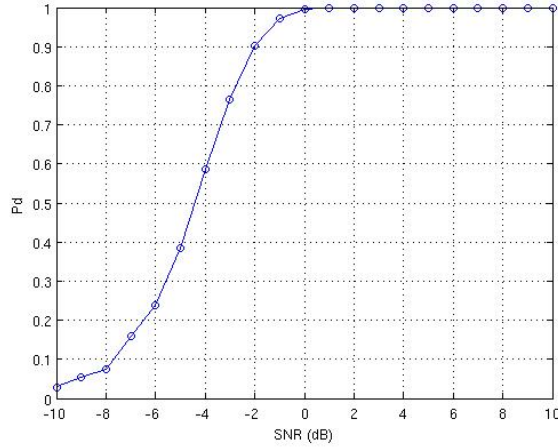


Figure 7: P_d against SNR_{pre} under Gaussian clutter for correlated subarrays. $P_{fa} = 10^{-3}$, $L_r = 3$, $K = 6$ and $N = 13$. MISO case.

between subarrays. Several different parameters were considered, e.g. the effective number of subarrays K and the effective number of elements N_e . On one hand, K can change N_e which in turn affects the SNR gain. On the other hand, it changes the threshold required to maintain the same P_{fa} . Monte-Carlo simulations are then carried out to compare the detection performance for different K .

For the adaptive version, we discussed the loss factor b which arises due to the estimation of the covariance matrix and the number of secondary data N_r required for satisfactory detection performance. Monte-Carlo simulations are then carried out to compare the detection performance for different K as well as for different N_r .

A. PROOF THAT THRESHOLD INCREASES WITH DEGREE OF FREEDOM

Proof. For a given P_{fa} and $\Lambda(\mathbf{y}) \sim \chi_{2K}^2(0)$:

$$\begin{aligned} P_{fa} &= P(\Lambda(\mathbf{y}) > \lambda | H_0) = \int_{\lambda}^{\infty} \frac{1}{2^K \Gamma(K)} x^{K-1} e^{-x/2} dx, \\ &= \frac{\Gamma(K, \frac{\lambda}{2})}{\Gamma(K)}, \end{aligned}$$

where $\Gamma(n, a)$ and $\Gamma(n)$ are the upper incomplete Gamma function and Gamma function, respectively. After modifying Eqn. (6.5.22) in [7], we have:

$$\Gamma(K, \frac{\lambda}{2}) = (K-1)\Gamma(K-1, \frac{\lambda}{2}) + (\frac{\lambda}{2})^{K-1} e^{-\lambda/2}.$$

As K is an integer, $\Gamma(K) = (K-1)!$ and hence:

$$\frac{\Gamma(K, \frac{\lambda}{2})}{\Gamma(K)} = \frac{\Gamma(K-1, \frac{\lambda}{2})}{\Gamma(K-1)} + \frac{(\frac{\lambda}{2})^{K-1} e^{-\lambda/2}}{\Gamma(K)}.$$

As the second term on the right hand side is positive, it means that given the same threshold λ , P_{fa} is bigger for bigger K . To keep P_{fa} constant, λ will have to be increased for bigger K . \square

REFERENCES

- [1] C. Y. Chong, F. Pascal, J-P. Ovarlez, and M. Lesturgie, "Robust MIMO radar detection for correlated subarrays," in *IEEE Int. Conf. on Acoustics, Speech and Sig. Proc. (accepted)*, Mar 2010.
- [2] E. Fishler, A. Haimovich, R. Blum, and L. J. Cimini, "Spatial diversity in radars - models and detection performance," *IEEE Trans. Sig. Proc.*, vol. 54, no. 54, pp. 823–838, March 2006.
- [3] N. H. Lehmann, A. Haimovich, R. Blum, and L. Cimini, "MIMO-radar application to moving target detection in homogeneous clutter," in *Proc. Adaptive Sensor Array Processing Workshop*, Lexington, USA, June 2006.
- [4] E. J. Kelly, "An adaptive detection algorithm," *IEEE Trans. Aero. Elect. Sys.*, vol. 22, no. 1, March 1986.
- [5] Kraut S, Scharf L L, and L T McWhorter, "Adaptive subspace detectors," *IEEE Trans. Sig. Proc.*, vol. 49, no. 1, Jan 2001.
- [6] T. W. Anderson, *An Introduction to Multivariate Statistical Analysis*, Wiley, 3rd edition, 2003.
- [7] M. Abramowitz and I. A. Stegun, *Handbook of Mathematical Functions*, National Bureau of Standard AMS 55, 1st edition, June 1964.